

# Theoretical prediction of compressive strength, Young's modulus and strain at fracture of sintered porous alumina compacts

Yoshihiro Hirata\*, Taro Shimonosono

Department of Chemistry, Biotechnology, and Chemical Engineering, Kagoshima University, 1-21-40 Korimoto, Kagoshima 890-0065, Japan

Received 8 October 2015; accepted 16 October 2015

Available online 23 October 2015

## Abstract

Young's moduli of sintered porous alumina compacts were theoretically related to the development of neck growth of grain boundary between sintered two particles. This model explained well the measured Young's moduli as a function of normalized grain boundary area determined from the specific surface areas of sintered alumina compacts. The theoretical compressive strength was also related to the grain boundary area and the number of grains in one sintered compact. The combined linear relationship between theoretical strength and theoretical Young's modulus gave the theoretical strain at fracture. The above calculation of mechanical properties provided a good approximation of the measured Young's moduli, compressive strengths and strains at fracture of sintered alumina compacts.

© 2015 Elsevier Ltd and Techna Group S.r.l. All rights reserved.

**Keywords:** Compressive strength; Young's modulus; Strain; Sintering; Porous ceramics

## 1. Introduction

Fracture of dense ceramics is well explained by linear fracture mechanics. The fracture strength depends on a fracture toughness and a flaw size [1]. Processing of structural ceramics aims at increase in the fracture toughness and decrease in the flaw size of its microstructure. On the other hand, a fracture strength of a porous ceramic material has been empirically related to its porosity [2] and has not been related theoretically to the characteristics of its microstructure. In our previous papers [3,4], it was proposed that the compressive strength ( $\sigma_f$ ) of a porous alumina ceramics is dominated by the grain boundary area ( $\pi y^2$ ) and the number of grain ( $N$ ) in a sintered porous alumina compact in Eq. (1),

$$\sigma_f = \sigma_0 \pi y^2 \left( \frac{N}{V} \right)^{2/3} \quad (1)$$

where  $\sigma_0$  ( $= 1.91$  GPa) and  $V$  are the compressive strength of a dense alumina ceramics without pores and the bulk volume of a sintered porous alumina ceramics, respectively. The  $y$  value

(i.e. radius of circular grain boundary in Fig. 1) is expressed by Eq. 2 [3],

$$y = 2^{2/3} r_0 \sqrt{\frac{2p - p^2}{(4 - 3np^2 + np^3)^{2/3}}} \quad (2)$$

where  $r_0$ ,  $n$  and  $p$  ( $= h/r$ ) are the radius of initial particle, the coordination number of particles and the ratio of the distance shrunk ( $h$ ) between two particles to the particle radius ( $r$ ), respectively. The  $p$  value is related to the area ( $A_{SV}$ ) of gas–solid interface in Fig. 1 by Eq. (3) [3].

$$A_{SV} = 4^{2/3} \pi r_0^2 \frac{4 - 2np}{(4 - 3np^2 + np^3)^{2/3}} \quad (3)$$

Thus the measurement of a specific surface area makes it possible to calculate the grain boundary area at a given coordination number of particles by Eq. (4).

$$\frac{S}{S_0} = \frac{A_{SV}}{A_0} = \frac{4 - 2np}{4^{1/3} (4 - 3np^2 + np^3)^{2/3}} \quad (4)$$

The  $S$  and  $S_0$  values represent the specific surface areas of alumina compacts after and before sintering, respectively. The  $A_0$  value is equal to the initial surface area ( $4\pi r_0^2$ ) of a spherical

\*Corresponding author. Tel.: +81 99 285 8325; fax: +81 99 257 4742.

E-mail address: [hirata@cen.kagoshima-u.ac.jp](mailto:hirata@cen.kagoshima-u.ac.jp) (Y. Hirata).

particle before sintering. The proposed models (Eqs. (1)–(4)) explained well the densification behavior and the compressive strengths for the alumina compacts sintered from well dispersed colloidal particles [3–5]. The consolidated microstructures were characterized by a random close packing structure (theoretical packing density 63.7%) with a coordination number  $n=12$ .

On the other hand, Young's modulus ( $E_c$ ) of a porous ceramic material was theoretically derived as a function of porosity in our recent paper [6]. Fig. 2(a) shows the model structure of material with cubic inclusion of size  $a$ . The number ( $p$ ) of inclusion along one direction of cubic composite is equal to  $V^{1/3}/a$  ( $V$ : volume fraction of inclusion) and the distance between two inclusion is given by  $(1/p-a)$ . The unit structure (Fig. 2(a)) was analyzed by the following two laminate model structures: a parallel structure model (Fig. 2(b)) of the rectangular composite (series connection of dispersed phase 1 and continuous phase 2) and the continuous phase 2 surrounding the rectangular composite, and a laminated series structure (Fig. 2(c)) of rectangular composite (parallel connection of dispersed phase 1 and continuous phase 2) and rectangular continuous phase 2. When the dispersed phase 1 is treated as pore (Young's modulus  $E_1=0$  GPa), the  $E_c$  values of parallel and series structures shown in

Fig. 2(b) and (c) are expressed in Eqs. (5) and (6), respectively [6],

$$E_c = E_2 \left( 1 - V_p^{2/3} \right) \quad (5)$$

$$\frac{1}{E_c} = \frac{V_p^{1/3} + \left( 1 - V_p^{1/3} \right) \left( 1 - V_p^{2/3} \right)}{E_2 \left( 1 - V_p^{2/3} \right)} \quad (6)$$

where  $E_2$  and  $V_p$  are Young's modulus of dense continuous phase 2 and the total porosity of open and closed pores, respectively. Eqs. (5) and (6) contain no specific experimental parameters and depends on only the porosity. Both the  $E_c$  values become  $E_2$  GPa for  $V_p=0\%$  and 0 GPa for  $V_p=100\%$ , respectively. In our recent paper [6], Young's modulus of the material with simple cubic particulate inclusion was derived and subsequently Young's modulus of the inclusion was treated to be 0 GPa for a porous material, giving Eqs. (5) and (6). The experimentally measured thermal expansion coefficients (TEC) of the W–MgO system were in accord with the calculated TEC based on the proposed mixing rule of Young's modulus for the series structure model. In this paper, the calculated Young's moduli (parallel and series structure models) for porous alumina compacts were compared with the measured data. Furthermore, the prediction of strain at fracture of porous alumina ceramics was discussed for the elastic deformation ( $\epsilon_f = \sigma_f / E_c$ , where  $\epsilon_f$  is the strain at fracture). A good agreement was observed between measured and predicted stress–strain curves of sintered porous alumina compacts.

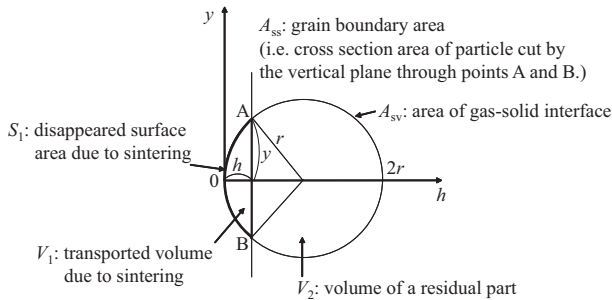


Fig. 1. Scheme of grain boundary development in sintered alumina powder compacts with uniform microstructures.

## 2. Experimental procedure

The detailed procedures of sample preparation and mechanical strength test were reported elsewhere [3–5]. Three types of  $\alpha$ - $\text{Al}_2\text{O}_3$  powders with different particle sizes were used to form alumina compacts ( $\text{Al}_2\text{O}_3$  purity > 99.99 mass%, Sumitomo Chemical Co. Ltd., Japan): AKP50 (specific surface area

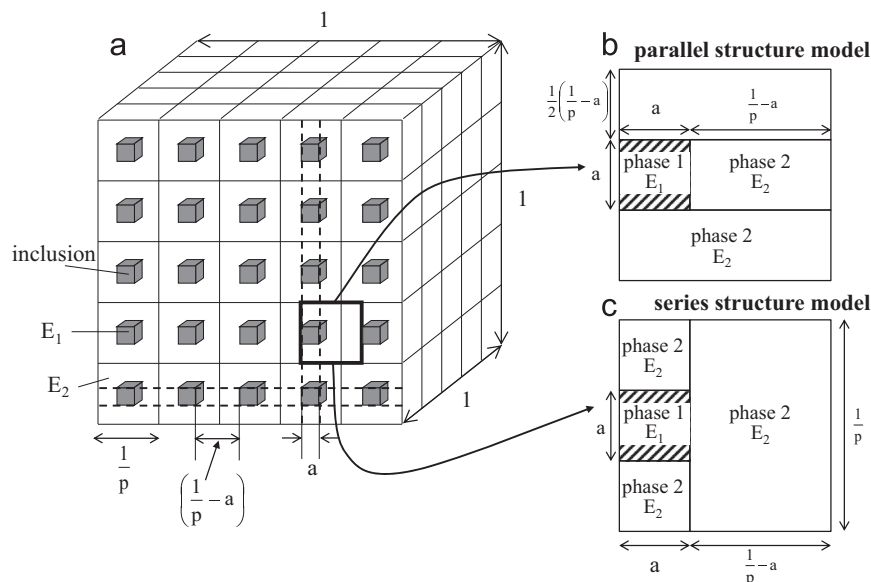


Fig. 2. (a) Structure of material with simple cubic inclusion with length  $a$ . The geometrical features are shown in (b) parallel and (c) series structure models.

Download English Version:

<https://daneshyari.com/en/article/1459516>

Download Persian Version:

<https://daneshyari.com/article/1459516>

[Daneshyari.com](https://daneshyari.com)